The Continental Margin is a Key Source of Iron to the HNLC North Pacific Ocean

Phoebe J. Lam[1,2] and James K.B. Bishop[2,3]

[1]Dept. of Marine Chemistry and Geochemistry, Woods Hole Oceanographic Institution, Woods Hole, MA 02540

[2]Earth Sciences Division, Lawrence Berkeley National Laboratory, Berkeley, CA 94720

[3]Dept. of Earth and Planetary Science, University of California, Berkeley, Berkeley, CA 94720

Abstract

Here we show that labile particulate iron and manganese concentrations in the upper 500m of the Western Subarctic Pacific, an iron-limited High Nutrient Low Chlorophyll (HNLC) region, have prominent subsurface maxima between 100-200 m, reaching 3 nM and 600 pM, respectively. The subsurface concentration maxima in particulate Fe are characterized by a more reduced oxidation state, suggesting a source from primary volcagenic minerals such as from the Kuril/Kamchatka margin. The systematics of these profiles suggest a consistently strong lateral advection of labile Mn and Fe from redox-mobilized labile sources at the continental shelf supplemented by a more variable source of Fe from the upper continental slope. This subsurface supply of iron from the continental margin is shallow enough to be accessible to the surface through winter upwelling and vertical mixing, and is likely a key source of bioavailable Fe to the HNLC North Pacific.

Keywords: iron, continental margin, HNLC

1. Introduction

The Subarctic Pacific is one of three major High Nutrient Low Chlorophyll (HNLC) regions of the world, where the paucity of the micronutrient iron limits biological productivity [*Boyd et al.*, 2004; *Tsuda et al.*, 2005]. Atmospheric dust deposition is commonly thought to be the primary mode of external iron supply to the open ocean [*Jickells et al.*, 2005]. Recent work, however, has shown that the continental margin of Alaska provides a subsurface supply of iron to the interior of the Eastern Subarctic Pacific that is important to productivity, particularly in the wintertime when dust flux is low and mixed layers are deep [*Lam et al.*, 2006].

The Western Subarctic Pacific (WSP) has higher biological productivity [*Harrison et al.*, 1999] and iron concentrations [*Nishioka et al.*, 2003; *Nishioka et al.*, 2007], and a stronger biological carbon pump [*Honda et al.*, 2006; *Buesseler et al.*, 2007] than the Eastern Subarctic Pacific. The higher WSP iron concentration is generally explained by its proximity to Asian dust sources and three-fold higher rates of dust deposition [*Mahowald et al.*, 2005]. Here we show that high subsurface concentrations of particulate iron observed in the WSP originate from the continental margin and rival the importance of dust.

2. Methods

Two pairs of profiles (casts 7-10) of size-fractionated suspended particles were collected over a 2-week period by the Multiple Unit Large Volume in-situ Filtration System [*Bishop et al.*, 1985] near station K2 (47°N, 161°W) in the center of the WSP gyre in July/August 2005 as part of the Vertical Transport in the Global Ocean (VERTIGO) project [*Buesseler et al.*, 2007].

Subsamples of the 1-51 μm size fraction were leached overnight in 0.6N HCl at 60°C [*Bishop et al.*, 1985] and the filtrate was run on a Finnegan Element II ICP-MS to determine concentrations of labile particulate Fe (Fe_P) and Mn (Mn_P). Total concentrations of Fe_P and Mn_P

(labile plus refractory silicate-bound phases) were determined using synchrotron x-ray fluorescence (XRF) at beamline 10.3.2 at the Advanced Light Source. Total Fe and Mn were determined by mapping the XRF counts over an area of 0.25mm^2 of the 1-51 μm size fraction filters at 10keV for Fe, and again at 6588 eV for Mn to avoid leakage into the Mn channel from Fe. XRF counts were quantified using NIST 1832,1833 thin-film XRF standards. The detection limit was defined as 3 times the standard deviation of Fe and Mn of a blank filter, and was 0.035 fmol Fe/μm^2 and 0.006 fmol Mn/μm^2. Total Fe_P and Mn_P concentrations were determined by summing all values above the detection limit after subtracting blank filter counts and dividing by the equivalent volume filtered through the mapped area.

The oxidation state of particulate Fe was determined by X-ray Absorption Near Edge Spectroscopy (XANES) using the position of the Fe-K pre-edge feature [*Wilke et al.*, 2001]. XANES data of the 1-51 μm size fraction were collected at the Stanford Synchrotron Radiation Laboratory at beamline 7-3 with a Si (220) monochromator in the fluorescence mode using a 30-element Ge detector array. Spectra were collected from ~200eV below to 300eV above the Fe K-edge (6900-7400eV), with 0.25 eV steps through the pre-edge region. XANES of an Fe foil was measured simultaneously in transmission mode to assure energy calibration. After the spectra were normalized (Fig. S1a), the pre-edge feature was extracted from the background (Fig. S1b). We used the relationship between the centroid position of the pre-edge peak (*C*) and redox ratio of mixtures of octahedrally-coordinated Fe minerals as determined by [*Wilke et al.*, 2001] (Table S1):

$$\frac{Fe^{3+}}{\Sigma Fe} \times 100 = \frac{0.0189 + \sqrt{3.582 \times 10^{-4} + 1.99 \times 10^{-4}\left(7112.1 - C\right)}}{10^{-4}}.$$

Variability in the particle field at different depths was determined during 13 CTD casts covering the period of MULVFS casts using a 25 cm path length C-Star transmissometer (WET Labs, Inc. Philomath, OR) with a 660 nm light source. The 24 Hz raw voltage transmissometer data were despiked and averaged every 10 s. Transmissometer profiles were drift corrected to bring voltages into match at 1000 m, where particle concentrations are very low and assumed invariant. Transmissometer voltages for all stations were binned by potential density (0.02 sigma theta bins), and the mean and standard deviation was determined for each bin. Particle beam attenuation coefficient (C_P) was derived from manufacturer's calibration procedures and at sea calibrations and was $C_P = -4\ ln(V - V_Z)/(V_{CW}-V_Z)$, where V is the despiked/drift corrected raw transmissometer voltage, V_Z is the blocked beam voltage, and $V_{CW} = 4.6729$ (voltage in particle free seawater). Most of the C_P signal is due to particulate organic matter [*Bishop et al.*, 2004].

3. Results and Discussion

Our WSP profiles from station K2 show that labile Mn_P and Fe_P concentrations rise rapidly with depth reaching peak concentrations (up to 600 pM Mn and 3 nM Fe) between 100 and 200 m; these levels are 6-times higher than at Ocean Station Papa (OSP) in the ESP (Fig. 1a,b). Deeper than 300 m, labile Mn_P and Fe_P are enhanced 3-fold relative to OSP.

The source of strongly elevated concentrations of acid-labile Mn_P in shallow waters is from the redox-driven remobilization of Mn^{+2} from shallow anoxic sediments of the continental shelf, and the subsequent precipitation of micron-sized Mn oxyhydroxide particles in oxygenated near-bottom waters, which are then transported offshore by subsurface currents [*Bishop and Fleisher*, 1987]. At station K2, Mn_P shows a distinct and reproducible subsurface maximum at 135 m in all WSP casts (Figure 1a). The total and labile Mn_P are nearly the same (Fig.1a), and the average total Mn_P:Fe_P ratio (~0.15) of our samples far exceeds crustal values (~0.017)

[*Taylor and McLennan*, 1995]. Further, the potential density surfaces at 135m on which the Mn_P peaks lie (σ_θ=26.61-26.69 kg/m^3) intersect the nearby Kuril/Kamchatka shelf (Fig. 2a). All lines of evidence thus point to a continental shelf origin for Mn_P in the WSP.

Labile Fe_P concentrations comprise ≥50% of total Fe_P and display subsurface maxima with peak values of 1-3 nM between 135m and 185m (Fig.1b). Fe_P at 185 m (σ_θ=26.7-26.8 kg/m^3) is significantly more variable than Mn_P at 135 m. The similarity with Mn_P but higher relative concentrations in deeper waters during two of the four casts suggests that a continental shelf source of Fe is supplemented by a variable upper continental slope source of Fe deeper down (Fig. 2b).

Numerous CTD/transmissometer profiles support this second and more variable deeper source. The particle beam attenuation coefficient, C_p, shows 9% variability at 185m, the depth of the variable peak in Fe_P, and only 3% variability at 135m, the depth of the relatively constant Mn_P (Fig. 3a). The higher variability in bulk particle field at the Fe_P peak is also seen when C_p is plotted against potential density (Fig. 3a). This supports the hypothesis that both the physical transport processes and sources for Fe_P originating from the upper continental slope are more variable. Hydrographic data further confirm the influence of different water masses at K2 during our occupation: temperature profiles around the first pair of MULVFS casts show a warmer temperature minimum and different deep structure than profiles taken ~10 days later, and potential density surfaces show displacements of ~40m in the depth interval 100-300m (Fig. 3b), suggesting passage of internal waves. Such strong variability is not surprising in this dynamic region of confluence of the Oyashio and Kuroshio currents.

The density surfaces on which the Mn_P and Fe_P peaks lie are shallower than the main oxygen minimum signal in intermediate waters (Fig. 2a). These density surfaces are consistent

with a source from the Sea of Okhotsk continental margin [*Nishioka et al.*, 2007], but the particulate Fe speciation data suggests a reduced Fe source. Determinations of the oxidation state of Fe_P showed that there is a distinct minimum in oxidation state (up to 25% Fe^{2+}) at 185m at the Fe_P concentration maximum (Fig. 1c). Since particulate iron from remobilized redox sources would likely have re-oxidized close to the sediment source, the presence of reduced iron suggests primary Fe-bearing minerals such as olivines and pyroxenes that are less weathered and more characteristic of a basaltic volcanic margin. Lithological maps clearly show that the Sea of Okhotsk margin is characterized by weathered clays and sands, whereas the Kuril/Kamchatka region is characterized by basalts [*Amiotte Suchet et al.*, 2003]. We thus hypothesize a consistently strong lateral advection of labile Mn_P and Fe_P at 135 m from redox-mobilized labile sources at the Kuril/Kamchatkan continental shelf to station K2 500 km offshore, supplemented by a more variable source of both redox-mobilized oxyhydroxides and mechanically resuspended refractory iron-silicates from the Kuril/Kamchatkan upper continental slope (Fig. 2b).

The overlap of elevated Fe_P at 135 m and the temperature minimum layer (Fig. 3b), which arises from surface cooling and deep wintertime mixing, suggests that this lateral source of Fe is shallow enough to be accessible by wintertime mixing. Further, high amplitude internal wave activity must augment this mixing since Fe is present in shallower waters.

The importance of a subsurface source of Fe compared to dust for primary productivity depends on the relative magnitude of the two fluxes to the euphotic zone and on the amount of bioavailable iron associated with each one. Annual dust deposition to the K2 area is estimated to be 0.3 $g/m^2/yr$ [*Measures et al.*, 2005], or 321μmol $Fe/m^2/yr$ for a 6% Fe content. Assuming a dust solubility of 4% [*Buck et al.*, 2006], this is 13 $\mu mol/m^2/yr$ of dissolved Fe from dust.

Several lines of argument suggest that the supply from below could be at least a comparable source of bioavailable Fe. First, the Fe bound in coastal sediments may be more inherently labile than Fe in dust: when subjected to comparable reducing and acidic leaching conditions (1 M hydroxalamine HCl at pH=2 for 18 hrs), Fe in suspended sediments from the Dutch Wadden Sea was 18% soluble [*Duinker et al.*, 1974] compared to 2% for Saharan aerosols [*Spokes et al.*, 1994]. While bulk seawater does not reach these leaching conditions, these conditions do exist in microenvironments such as within organic aggregates (marine snow) and in the guts of grazers [*Barbeau et al.*, 1996].

Second, dissolved Fe (Fe_D) likely accompanies the elevated subsurface Fe_P that we measure. Labile Fe_P from the margin originally precipitated from an excess in the concentration of Fe_D over organic Fe-binding ligands in Fe-rich coastal waters [*Buck et al.*, 2007], and models have shown the lateral advection of both Fe_D and Fe_P from coastal regions to the open ocean in the Subarctic Pacific [*Lam et al.*, 2006; *Moore and Braucher*, 2007]. Indeed, Fe_D profiles taken by other investigators at stations close to K2 in the WSP show a rapid increase in Fe_D to concentrations of 0.8-0.9 nM at the depth of our Fe_P and Mn_P peaks (Station KNOT: 47°N, 155°E [*Nishioka et al.*, 2003] and IOC 2002 Stn 3: 50°N, 167°E [*Brown et al.*, 2005], Fig. 2a). When Fe_P data were measured, the Fe_D increase was accompanied by a distinct 1.0 nM maximum in labile Fe_P at 140 m [*Nishioka et al.*, 2003; *Nishioka et al.*, 2007]. Any upwelling or vertical mixing would thus bring both Fe_P and Fe_D to the surface.

We can estimate the annual vertical supply of Fe_D and labile Fe_P to the surface mixed layer from upwelling and vertical diffusivity. The K2 area has little Ekman upwelling in the summer (April-September), but high upwelling (0.043 m/d at the base of the mixed layer) in the winter (October-March) [*Bograd et al.*, 1999]. We take the more offshore IOC 2002 Stn 3 Fe_D

profile [*Brown et al.*, 2005] as a conservative estimate for the Fe_D profile at Station K2, and make the assumption that the summertime labile Fe_P and Fe_D profiles are representative of year-round conditions. Using concentrations of 1.3 nM Fe_P (average of 4 casts, Fig. 1b) and 0.6 nM Fe_D [*Brown et al.*, 2005] at 135 m, which we take as the depth of the winter mixed layer deduced from base of the temperature minimum, we estimate a vertical upwelling supply of 56 nmol $Fe_P/m^2/d$ and 26 nmol $Fe_D/m^2/d$ in the winter, or 10.2 μmol $Fe_P/m^2/yr$ and 4.7 μmol $Fe_D/m^2/yr$. Estimates for vertical eddy diffusivity range from ~1-10 m^2/d [*Talley*, 1995]. Assuming a middle range vertical diffusivity of 5 m^2/d and a gradient of 13 nmol Fe_P/m^4 and 6 nmol Fe_D/m^4 between 35 and 135 m, we estimate a vertical mixing supply of 65 nmol $Fe_P/m^2/d$ and 30 nmol $Fe_D/m^2/d$, or 24 μmol $Fe_P/m^2/yr$ and 11 μmol $Fe_D/m^2/yr$. Assuming that only 2% of the labile Fe_P is bioavailable and all Fe_D is bioavailable, this sums to a total vertical delivery from upwelling and vertical diffusivity of 16 $\mu mol/m^2/yr$ of bioavailable iron, comparable to the 13 $\mu mol/m^2/yr$ of dissolved Fe from dust, and which would increase at higher levels of Fe_P bioavailability.

4. Conclusions

The observed variability in optically sensed particles, hydrography, profile systematics of Mn_P and Fe_P, and Fe_P speciation argue for a dynamically controlled lateral source of biologically important metals from a nearby volcanic continental margin rather than from dust. Fe_P is not only a tracer for the delivery of total Fe that includes dissolved Fe, but also retains the memory of its source through its chemical speciation. Simple calculations show that subsurface Fe delivery from the shelf is likely as important a source of bioavailable iron to the HNLC WSP gyre than dust. This mechanism of subsurface iron delivery may also important to other HNLC regions downstream of continental shelves.

Acknowledgements

We thank S. Bone, M. Marcus, and T. Wood for help analyzing samples at the ALS and LBL, J.M. Lee for help at SSRL, and helpful comments from three reviewers. Funding from the US Department of Energy, Office of Science, Biological and Environmental Research Program (JB) and WHOI Postdoctoral Scholars program, the Richard B. Sellars Endowed Research Fund, and the Andrew W. Mellon Foundation Endowed Fund for Innovative Research (PL). The Advanced Light Source is supported by the Director, Office of Science, Office of Basic Energy Sciences, of the U.S. Department of Energy under Contract No. DE-AC02-05CH11231. Portions of this research were carried out at the Stanford Synchrotron Radiation Laboratory, a national user facility operated by Stanford University on behalf of the U.S. Department of Energy, Office of Basic Energy Sciences.

References

Amiotte Suchet, P., J. Probst, and W. Ludwig, Worldwide distribution of continental rock lithology: Implications for the atmospheric/soil CO2 uptake by continental weathering and alkalinity river transport to the oceans, *Global Biogeochemical Cycles*, *17* (2), 1038,2003.

Barbeau, K., J. W. Moffett, D. A. Caron, P. L. Croot, and D. L. Erdner, Role of protozoan grazing in relieving iron limitation of phytoplankton, *Nature*, *380* (6569), 61-64,1996.

Bishop, J. K. B., and M. Q. Fleisher, Particulate Manganese Dynamics in Gulf-Stream Warm-Core Rings and Surrounding Waters of the Nw Atlantic, *Geochimica Et Cosmochimica Acta*, *51* (10), 2807-2825,1987.

Bishop, J. K. B., D. Schupack, R. M. Sherrell, and M. Conte, A Multiple-Unit Large-Volume In-situ Filtration System for Sampling Oceanic Particulate Matter in Mesoscale Environments, *Advances in Chemistry Series* (209), 155-175,1985.

Bishop, J. K. B., T. J. Wood, R. E. Davis, and J. T. Sherman, Robotic observations of enhanced carbon biomass and export at 55 degrees S during SOFeX, *Science*, *304* (5669), 417-420,2004.

Bograd, S. J., R. E. Thomson, A. B. Rabinovich, and P. H. LeBlond, Near-surface circulation of the northeast Pacific Ocean derived from WOCE-SVP satellite-tracked drifters, *Deep-Sea Research Part Ii-Topical Studies in Oceanography*, *46* (11-12), 2371-2403,1999.

Boyd, P. W., et al., The decline and fate of an iron-induced subarctic phytoplankton bloom, *Nature*, *428* (6982), 549-553,2004.

Brown, M. T., W. M. Landing, and C. I. Measures, Dissolved and particulate Fe in the western and central North Pacific: Results from the 2002 IOC cruise, *Geochemistry Geophysics Geosystems*, *6*,2005.

Buck, C. S., W. M. Landing, J. A. Resing, and G. T. Lebon, Aerosol iron and aluminum solubility in the northwest Pacific Ocean: Results from the 2002 IOC cruise, *Geochemistry Geophysics Geosystems*, *7*,2006.

Buck, K. N., M. C. Lohan, C. J. M. Berger, and K. W. Bruland, Dissolved iron speciation in two distinct river plumes and an estuary: Implications for riverine iron supply, *Limnology and Oceanography*, *52* (2), 843-855,2007.

Buesseler, K. O., et al., Revisiting carbon flux through the ocean's twilight zone, *Science*, *316* (5824), 567-570,2007.

Duinker, J. C., G. T. M. Van Eck, and R. F. Nolting, On the behaviour of copper, zinc, iron, and manganese, and evidence for mobilization processes in the Dutch Wadden Sea, *Netherlands Journal of Sea Research*, *8* (2-3), 214-239,1974.

Harrison, P. J., P. W. Boyd, D. E. Varela, and S. Takeda, Comparison of factors controlling phytoplankton productivity in the NE and NW subarctic Pacific gyres, *Progress in Oceanography*, *43* (2-4), 205-234,1999.

Honda, M. C., H. Kawakami, K. Sasaoka, S. Watanabe, and T. Dickey, Quick transport of primary produced organic carbon to the ocean interior, *Geophysical Research Letters*, *33*, doi:10.1029/2006GL026466,2006.

Jickells, T. D., et al., Global iron connections between desert dust, ocean biogeochemistry, and climate, *Science*, *308* (5718), 67-71,2005.

Lam, P. J., J. K. B. Bishop, C. C. Henning, M. A. Marcus, G. A. Waychunas, and I. Y. Fung, Wintertime phytoplankton bloom in the subarctic Pacific supported by continental margin iron, *Global Biogeochemical Cycles*, *20* (1), doi:10.1029/2005GB002557,2006.

Mahowald, N. M., A. R. Baker, G. Bergametti, N. Brooks, R. A. Duce, T. D. Jickells, N. Kubilay, J. M. Prospero, and I. Tegen, Atmospheric global dust cycle and iron inputs to the ocean, *Global Biogeochemical Cycles*, *19* (4), doi:10.1029/2004GB002402,2005.

Measures, C. I., M. T. Brown, and S. Vink, Dust deposition to the surface waters of the western and central North Pacific inferred from surface water dissolved aluminum concentrations, *Geochemistry Geophysics Geosystems, 6*,2005.

Moore, J. K., and O. Braucher, Sedimentary and mineral dust sources of dissolved iron to the World Ocean, *Biogeosciences Discussion, 4* (2), 1279-1327,2007.

Nishioka, J., et al., Iron supply to the western subarctic Pacific: Importance of iron export from the Sea of Okhotsk, *Journal of Geophysical Research-Oceans, in press*,2007.

Nishioka, J., S. Takeda, I. Kudo, D. Tsumune, T. Yoshimura, K. Kuma, and A. Tsuda, Size-fractionated iron distributions and iron-limitation processes in the subarctic NW Pacific, *Geophysical Research Letters, 30* (14), doi:10.1029/2002GL016853,2003.

Schlitzer, R., Ocean Data View,1996.

Spokes, L. J., T. D. Jickells, and B. Lim, Solubilization of Aerosol Trace-Metals by Cloud Processing - a Laboratory Study, *Geochimica Et Cosmochimica Acta, 58* (15), 3281-3287,1994.

Talley, L. D., Some advances in understanding of the general circulation of the Pacific Ocean, with emphasis on recent U.S. contributions, in *U.S. National Report to IUGG, 1991-1994*, edited by R. Pielke, American Geophysical Union, 1995.

Taylor, S. R., and S. M. McLennan, The Geochemical Evolution of the Continental-Crust, *Reviews of Geophysics, 33* (2), 241-265,1995.

Tsuda, A., et al., Responses of diatoms to iron-enrichment (SEEDS) in the western subarctic Pacific, temporal and spatial comparisons, *Progress in Oceanography, 64* (2-4), 189-205,2005.

Wilke, M., F. Farges, P. E. Petit, G. E. Brown, and F. Martin, Oxidation state and coordination of Fe in minerals: An FeK-XANES spectroscopic study, *American Mineralogist, 86* (5-6), 714-730,2001.

Figure captions.

Fig. 1: Concentration profiles of particulate **(a)** Mn and **(b)** Fe as determined by ICP-MS on the acid leachable (labile) fraction (solid line), and by synchrotron XRF (total) (dashed lines, grey symbols) in the 1-51 μm particle size fraction. Acid-leachable concentrations from Ocean Station Papa (OSP) in the ESP [*Lam et al.*, 2006] shown (solid lines, X symbols) for comparison. Error bars on XRF Fe, where present, indicate standard deviations of samples analyzed twice. **(c)** Profiles of the redox ratio of particulate Fe, expressed as $Fe^{3+}/\Sigma Fe*100$, showing a minimum in oxidation state at 185m. See Table S1 for analysis details. The depths/densities of Mn and Fe maxima are shown as large horizontal dashes in all profiles.

Fig. 2: (a) Potential density (thick contours) and dissolved oxygen (thin contours) sections constructed from three WOCE cruises connecting the Kamchatka peninsula (right third: P13-August 1992), station K2 (vertical dashed line; middle third: P1-August 1985), and into the Sea of Okhotsk through the Kuril Straights (left third: P01W-September 1993) [*Schlitzer*, 1996], showing that the density surfaces on which the Mn (x) and Fe (x') peaks lie intersect with the continental shelf and upper continental slope of Kamchatka and the Kuril Islands and are shallower than the core of the oxygen minimum zone (20 μmol/kg). This composite section is merely illustrative and is not meant to imply a particular pathway for delivery of Mn and Fe. Locations of closest available dissolved Fe profiles from [*Nishioka et al.*, 2003] and [*Brown et al.*, 2005] marked with *. **(b)** Schematic of Mn and Fe delivery from continental shelf and slope to open ocean, showing constant shelf source of remobilized Mn and Fe from the shelf, and a more variable source of Fe remobilized and resuspended from reducing slope sediments.

Fig. 3: Data from 13 CTD profiles bracketing pairs of MULVFS casts: 1st set (Jul 30-Aug 2) shown as open circles; 2nd set (Aug 10-12 2005) shown as smaller closed triangles. **(a)** Particle beam attenuation coefficient (C_p) plotted against depth (left) and potential density (right)

showing more variable particle concentrations above and below 135 m. Mn_P and Fe_P phases are minor contributors to the C_p signal which is dominated by organic matter [*Bishop et al.*, 2004]. *Cp* values in waters shallower than 50 m were as high as 0.2 (not shown). **(b)** Depth profiles of temperature (symbols) and potential density (solid and dotted lines denote depth range of potential density surfaces during the 1st and 2nd sets, respectively). Isopycnal displacements of ~40 m were evident in the 1st set. The relatively large variability for Fe near 185 m is consistent with C_p data and indicates a more variable upper continental slope source. Dust delivered material would not exhibit such depth dependent variability.

Figure 1

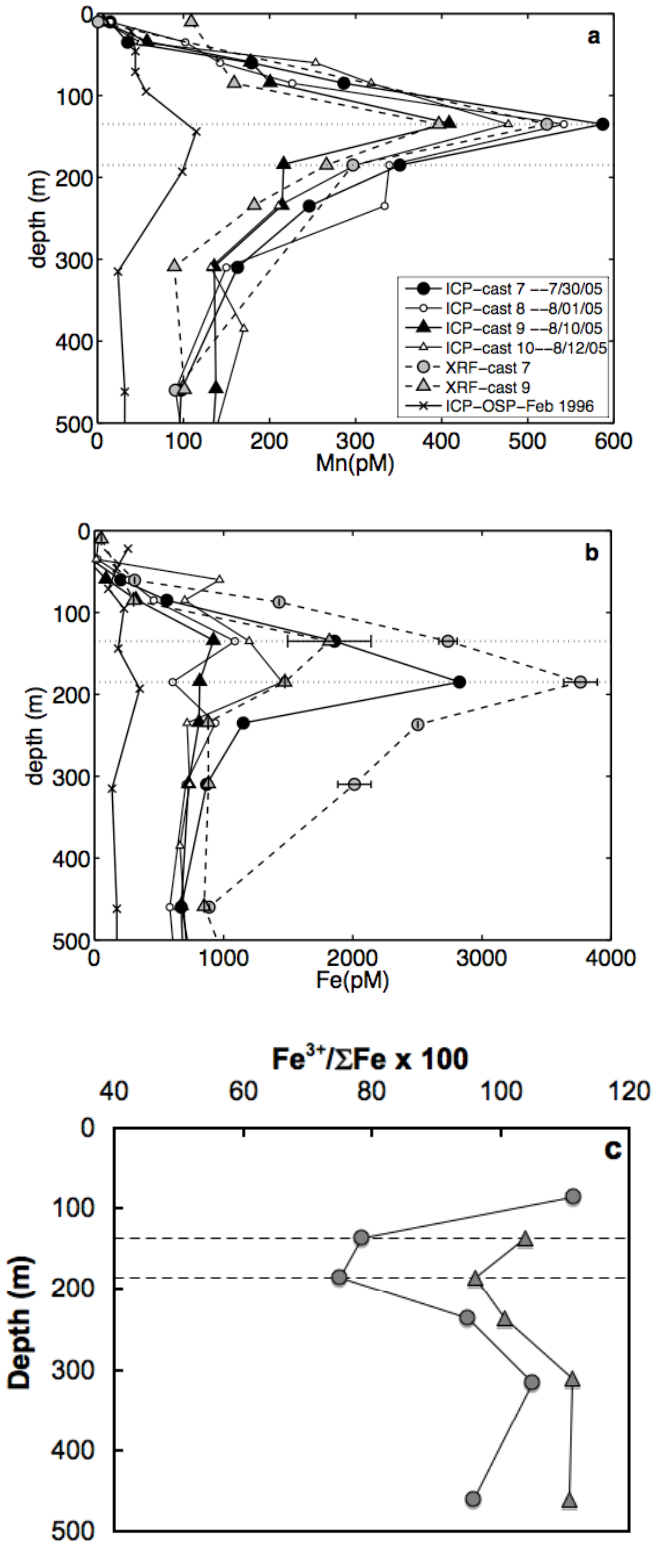
a
depth (m)
Mn(pM)
ICP−cast 7 −−7/30/05
ICP−cast 8 −−8/01/05
ICP−cast 9 −−8/10/05
ICP−cast 10−−8/12/05
XRF−cast 7
XRF−cast 9
ICP−OSP−Feb 1996
b
depth (m)
Fe(pM)
Fe3+/ΣFe x 100
c
Depth (m)

Figure 2

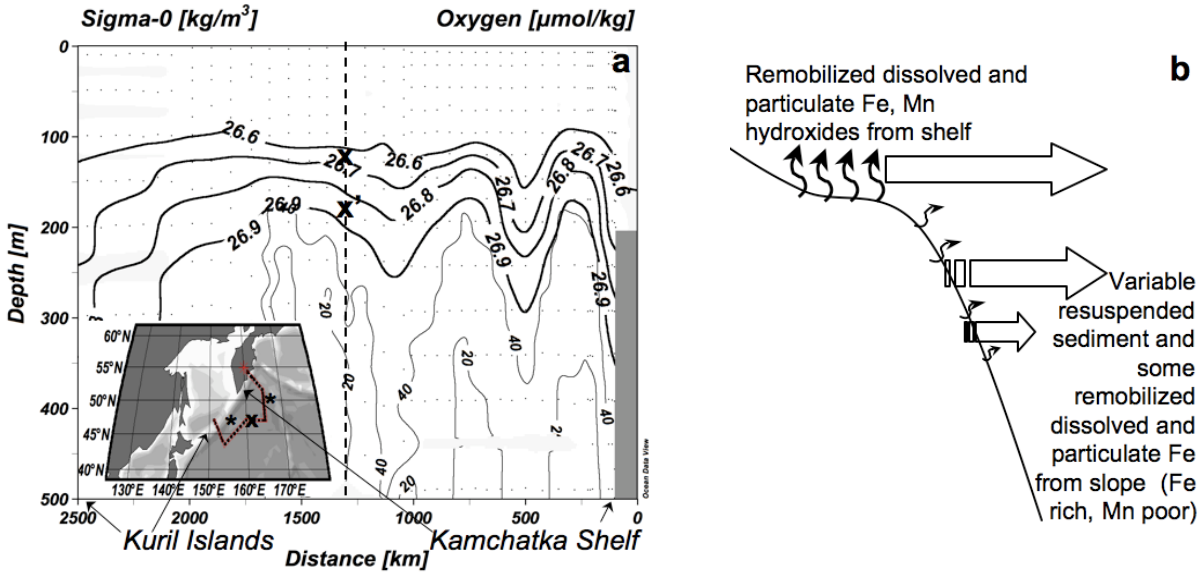

Figure 3